A spatio-temporal multiplexing multi-view display using a lenticular lens and a beam steering screen

Xiangyu Zhang, Weitao Song *, Hongjuan Wang, Zhenfeng Zhuang, Phil Surman, Xiao Wei Sun, Yuanjin Zheng

Advanced Display Lab, School of Electrical and Electronic Engineering, Nanyang Technological University, 50 Nanyang Avenue, 639798, Singapore

ARTICLE INFO

Keywords:
Autostereoscopic displays
Steering screens
Multi-view displays

ABSTRACT

A new type of spatio-temporal multiplexing multi-view three-dimensional (3D) display with horizontal motion parallax has been developed. The proposed 3D display system comprises: a fast liquid-crystal-display (LCD), a lenticular lens and a beam steering screen. The lenticular lens is customized for the LCD screen so as to project the display image into different directions. The beam steering screen is fabricated by using two layers of twisted-nematic (TN) LC cells with micro-prism-array(MPA) substrates, and multiple polarization statues can be produced by regulating the biasing voltages on the steering screen. Image light beam from the LCD screen is firstly split by the lenticular lens, and then further deflected to desired directions by the steering screen. Thus, the proposed method implements temporal multiplexing onto common spatial multiplexing multi-view displays, and dense viewing zones are created horizontally in space. A complete prototype based on this technology has been developed, and the proof of concept has been verified by experimental results.

1. Introduction

Unprecedented progress in three-dimensional (3D) displays has been witnessed over past two decades. Conventional binocular 3D displays are implemented by wearing special glasses to view disparate images in two eyes of viewers [1]. In comparison with the binocular stereo technology, an autostereoscopic display is more appealing as it does not require viewers to wear any glasses or headgear. Existing autostereoscopic technologies can be categorized into four basic classes including holographic displays [2,3], volumetric displays [4,5], light field displays [6–8] and multi-view displays [9–11].

Holographic displays have potential to provide the most realistic 3D sensation with a perfect reproduction of both amplitude and phase on original scenes. However, this approach involves a huge amount of data processing on image acquisition, transmission and display [12]. Even if the enabling technology eventually can provide the vast processing power required, the practical implementation of holographic displays is still challenging [13,14]. A 3D image can be constructed within a number of predefined voxels in volumetric displays. Although semi-transparent natural-looking 3D imagery can be reconstructed in an actual space, correct light angular distribution and occlusion cannot be easily achieved due to fundamental limitations in principle. In light field displays, abundant different light rays should be precisely reconstructed to ensure that they enter the viewer's pupils from two or more different perspectives so as to provide correct depth cues, thus it requires a tremendous amount of computation on a huge amount of image data to achieve a true 3D image, which prevents the technology from practical usage at present.

Multi-view displays can provide a series of viewing zones in space and have the potential to achieve super multi-view displays by increasing the number of viewing zones. Multi-view display technology can be classified into two categories in the spatial and temporal domains. Spatial multiplexing can be simply implemented by low-cost parallax barriers or lenticular sheets in conjunction with liquid-crystal-displays (LCD) or projectors [15,16]. However, this technique suffers from the loss of spatial resolution to each viewer, and it only provides limited depth of field. Resolution reduction can be alleviated to a certain extent by employing a slanted lenticular structure in which the resolution loss is redistributed in both horizontal and vertical directions [17]. This improvement makes spatial multiplexing 3D displays commercially available. Unfortunately, it is still unfeasible to achieve a practical 3D display with a sufficient number of viewing zones and an adequate resolution for every viewer simultaneously by using spatial multiplexing alone. Temporal multiplexing sequentially directs the display image on a fast screen into different viewing positions. There are many approaches

* Corresponding author.
E-mail address: bitsongweitao@gmail.com (W. Song).

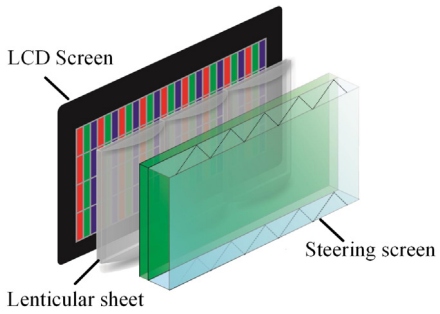

Fig. 1. System architecture of the spatio-temporal multiplexing multi-view display.

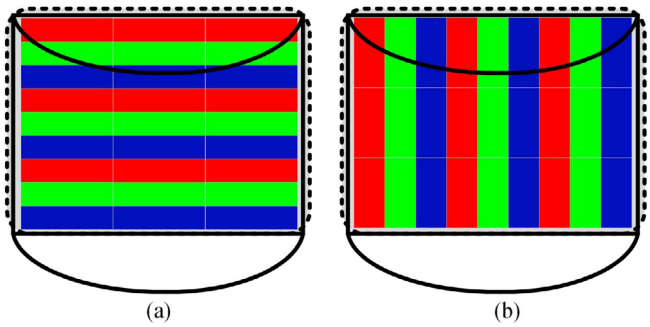

Fig. 2. (a) pixel arrangement in a lenticular based 3-view display, (b) narrow pixel structure in the proposed spatio-temporal multiplexing multi-view display. (For interpretation of the references to color in this figure legend, the reader is referred to the web version of this article.)

to realize temporal multiplexing with diverse light sources, and these include but not limited to a high-speed projector [18], a scanning laser [19] and a light-emitting-diode (LED) array [20]. However, the complex optical design requires precise alignment on a bulky system with an extreme hardware cost, which prevents them from commercial applications.

In this paper, a new type of multi-view 3D display is proposed, where spatial and temporal multiplexing are implemented in the same display system. The proposed 3D display comprises a fast LCD screen, a lenticular lens and a beam steering device. The lenticular lens is customized for the LCD panel so that the display image on the screen is horizontally split and projected into multiple directions. A beam steering device has been designed based on two layers of twisted-nematic (TN) LC cells and micro-prism-array (MPA) substrates, which can deflect incident light beams to different directions by varying the biasing voltages on LC cells. Since the beam steering screen is mounted in front of the lenticular sheet, the proposed 3D display implements temporal multiplexing onto a spatial multiplexing structure. Compared with conventional multi-view displays with lenticular lens, the adoption of the TN LC cells can increase the number of views by the temporal-multiplexing method. On the other hand, the size of developed temporal-multiplexing multi-view display is dramatically reduced because the TN LC cells are thin and compact. In the field of 3D displays, the requirements of the speed and resolution of display devices could also be challenging, and the trade-off still exists between the performance and cost in the practical implementations. The number of separate views will be determined by the product of the number provided by the spatial-multiplexing method and the one provided by the temporal-multiplexing methods. The proposed technology has the potential to provide an abundant number of separate viewing zones by balancing the spatial-multiplexing and temporal-multiplexing methods while maintaining a compact size.

The rest of the paper is organized as follows: Section 2 describes the principle of the proposed spatio-temporal multiplexing multi-view 3D display system; Section 3 presents the design of lenticular lens with measurement results; The development of a beam steering device is presented in Section 4; Section 5 describes the system level implementation of the prototype; Experimental results are summarized in Section 6, and Section 7 is the conclusion.

2. System architecture

The system architecture of the spatio-temporal multiplexing multi-view display is shown in Fig. 1, where there are three main components including: a fast display, a lenticular sheet and a beam steering screen. These devices are cascaded with the lenticular sheet being accurately aligned with the rear display.

In a lenticular based multi-view display, the width of each viewing zone is directly proportional to the pixel pitch. In order to achieve more viewing zones, a narrow pixel structure is proposed in this paper. Fig. 2(a) shows an example of the pixel arrangement in a conventional lenticular based 3-view display where each lens covers three pixels, and every column is assigned to a single view. The proposed narrow pixel structure is illustrated in Fig. 2(b) where the lenticular lens is placed parallel with color columns. It can be noted that lenticular lenses in Fig. 2(a) and (b) have the same spatial dimension. However, the horizontal pixel in Fig. 2(b) is much narrower, and thus the lenticular lens in this design can provide three times more viewing zones than that in Fig. 2(a).

In order to evaluate the spatio-temporal multiplexing technology, a 9-view display system is developed based on the proposed structure in Fig. 1. In this prototype, as shown in Fig. 2(b), every lenticular lens covers nine sub-pixels, and there are nine repeating viewing zones created in the horizontal space. However, in a given viewing position, only a monochrome image can be observed. In order to provide full color images, a temporal multiplexing technology is developed to elaborately shift images among the entire viewing field in sequence, and thus every viewer can continuously observe separate red, green and blue images.

Spatio-temporal multiplexing can be explained by Fig. 3, where a complete display cycle T comprises three sub-cycles ($T_1, T_2, T_3 = 1/3T$). A frame of a full color image (*Image*) is split into three disparate frames of sub-images ($Image_1$, $Image_2$ and $Image_3$), which are precisely synchronized with sub-cycles (T_1, T_2, and T_3) in time domain. By periodically regulating the biasing voltage on the steering screen, light beams from the lenticular sheet are deflected into three discrete angles ($Angle_1$, $Angle_2$ and $Angle_3$) through the entire viewing plane in sequence. For the sake of simplicity, the viewing position (V_5) is chosen as an example for analysis. In the first sub-cycle T_1, the LCD screen shows the sub-image ($Image_1$), and the steering screen works in the deviation angle ($Angle_1$). Consequently, at the V_5 viewing position, an observer can only perceive a green monochrome image projected from the whole screen. In the second sub-cycle T_2, the image on the LCD screen is switched into another sub-image ($Image_2$), at the same time, the steering screen is configured into the deflection angle ($Angle_2$). As a result, only a red monochrome image is projected to the V_5 viewing position. The last sub-cycle works in the same way by creating a blue monochrome image at the V_5 viewing position. Therefore, within a complete frame cycle, three primary color sub-images are displayed sequentially at the same position. The human visual system fuses these sub-images into the appearance of a full color image.

3. Lenticular sheet

In a conventional lenticular based autostereoscopic display, a lenticular sheet is directly attached to a display screen, and each cylindrical lens cell covers multiple sub-pixel columns. Since sub-pixels on the display panel are located at the focal plane of the lenticular sheet, they are magnified by the lens to form separate viewing zones at a certain distance, referred as the optimum viewing distance. The number of the

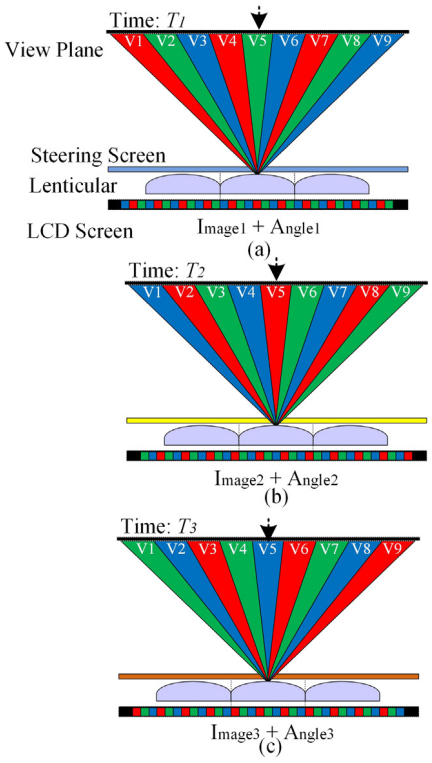

Fig. 3. Demonstration of the spatio-temporal multiplexing 9-view display system in a complete display cycle. (For interpretation of the references to color in this figure legend, the reader is referred to the web version of this article.)

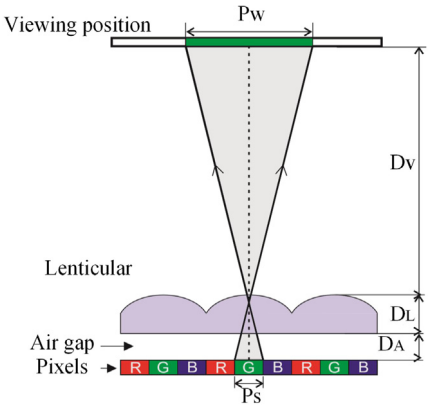

Fig. 4. Viewing zone formation on the air-gap lenticular sheet. In this example, the number of the viewing zone is three.

Table 1
Parameters for lenticular screen.

Parameter	Value
Number of views k	9
Pixel size	276.75 μm × 276.75 μm (RGB)
Lenticular screen size	531.36 mm (H) × 298.89 mm (V)
Sub-pixel pitch P_s	92.25 μm
Refractive index N_L	1.56
Viewing zone width P_W	20 mm
Optimum viewing distance D_V	1200 mm
Thickness of substrate D_D	2 mm
Radius of lens R	3109.6 μm
Height of lens D_L	27.5 μm
Pitch of lens P_L	826.6 μm
Air gap D_A	4.2 mm

viewing zones equals to the number of sub-pixels covered by each lens. In order to reduce the weight of the lenticular sheet in the proposed prototype, it is designed to be mounted with an air gap as shown in Fig. 4.

The viewing zone formation based on the proposed lenticular sheet is illustrated in Fig. 4. The optical magnification factor M is defined as the ratio between the width of the viewing zone P_W and the sub-pixel pitch P_S, which is given as follows:

$$M = \frac{P_W}{P_S}. \tag{1}$$

Based on a geometrical approximation at the optimum viewing distance shown in Fig. 4, the air gap D_A between the lenticular sheet and the display screen can be calculated by the following expression.

$$D_A = \frac{D_V}{M} - \frac{D_L}{N_L} \tag{2}$$

where D_V is the optimum viewing distance while D_L and N_L correspond to the thickness and refractive index of the lenticular screen respectively.

The effective distance F of the lens cell is given as follows:

$$F = D_A + \frac{D_L}{N_L} + D_D \tag{3}$$

where D_D is the thickness of the glass substrate on the lenticular screen.

Thus, the radius R of the lenticular screen can be given as below:

$$R = F \times \left(N_L - 1\right). \tag{4}$$

In order to get a magnified image at the optimum viewing position, the lens width should be slightly smaller than the sub-pixel pitch, and it can be calculated as follows:

$$P_L = \frac{k \times P_S \times M}{(M+1)} \tag{5}$$

where k denotes the desired number of viewing zones. Therefore, based on above equations, the lenticular sheet is designed with appropriate parameters, which are summarized in Table 1.

An experimental system has been set up to measure the performance of the multi-view display system with a lenticular. Fig. 5(a) shows the experimental set-up, and an Eldim VCmaster 3D analyzer was employed to measure the angular luminance distribution over the entire viewing field. An example testing image pattern is input to the display screen to characterize the luminance distribution on viewer V_1 positions, which is shown in Fig. 5(b). Under this pattern, only the viewing zone V_1 receives a red monochrome image while the rest of viewing zones are set in a dark condition. For the other eight views, the illumination distribution can be measured in the same manner by applying appropriate testing image patterns. The angular luminance distributions for one cycle of nine separate views are summarized in Fig. 5(c), and it shows that the nine viewing zones are discretely separated. The crosstalk has been discussed in literature works, and in our work the crosstalk is defined as the ratio of the luminance leakage to the whole luminance at the best view position. Here, the luminance leakage is the amount of light that leaks from other stereoscopic views to the correct one. Based on the data measured by the Eldim VCmaster 3D analyzer (shown in Fig. 5(c)), the averaged crosstalk for these selected nine views is 23.8%, and the largest crosstalk among the nine views is 25.3%. The crosstalk is generated due to the misalignment and the machining tolerance of the optical elements. It should be pointed out that the main purpose of the work is to propose a new spatio-temporal multiplexing multi-view display; thus, a commercial lenticular lens was used which was not optimized or custom-built. The performance can be further improved if the optical elements are best chosen and the rendering algorithm is improved, nevertheless, it is out of the main scope of this work and will be reported somewhere.

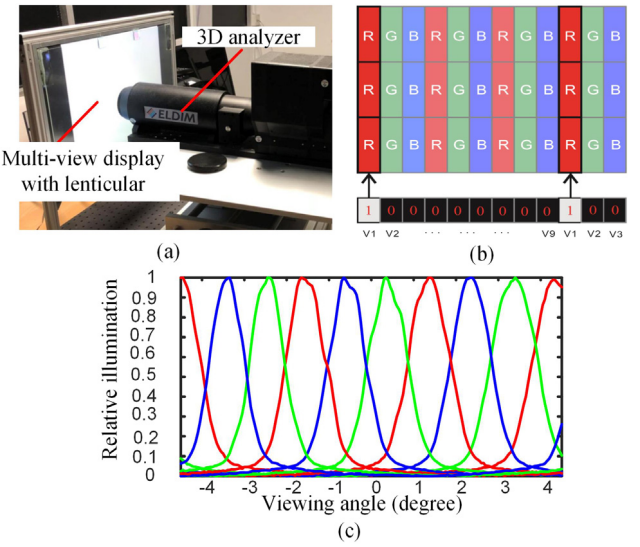

Fig. 5. (a) Experimental set-up. (b) An example testing image pattern for the viewing zone. (c) Experimental results. (For interpretation of the references to color in this figure legend, the reader is referred to the web version of this article.)

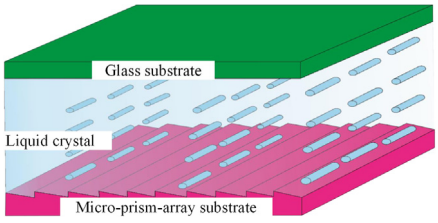

Fig. 6. Structure on the liquid crystal micro-prism-array (MPA) device.

4. Steering screen

Traditional steering devices tend to be mechanical methods such as micro lenses, micro-mirrors or linear arrays. Such mechanical approaches are constrained by the response speed as they require a long period to react. In this paper, a non-mechanical beam steering device is developed, and it is capable of deflecting any incident light by the same angle. By cascading the steering device with the lenticular sheet, images split from the display screen can be shifted in discrete steps through the entire viewing space, which physically implements the temporal multiplexing function. The proposed steering screen comprises two components: a polarization rotator and a birefringent prism. The polarization rotator is used to rotate incident light by 90° when necessary. With appropriate alignment of prism facets, the birefringent prism can deflect the incident light with two specific angles which are determined by incident light polarization states.

In this paper, the polarization rotator is developed by a wavelength-independent TN LC cell which solely switches between two alternative states. In absence of a driving voltage, the TN LC works in its linear polarization mode which inherently rotates incident light by 90°. With an appropriate driving voltage, incident light will not be rotated when it passes through the TN LC cell. In this prototype, the birefringent prism is implemented by passive liquid crystal materials. As shown in Fig. 6, the main building blocks of the birefringent prism include a glass substrate with a liquid crystal filled gap and a micro-prism-array (MPA) substrate. This device has two different deflection directions: one for the ordinary-ray (O-ray) and one for the extraordinary-ray (E-ray). Since the light polarization switching between O-ray and E-ray is regulated

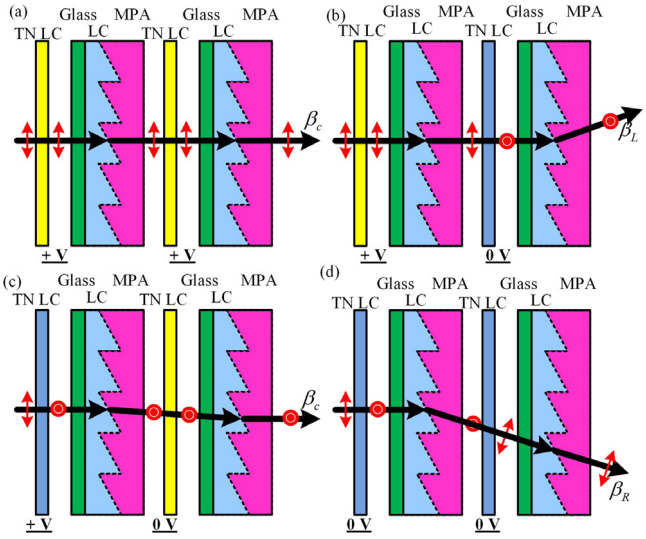

Fig. 7. Operating statuses on the beam steering screen.

by the front-end TN LC rotator, incident light beams can be deflected into different directions by applying appropriate driving voltages onto the beam steering device.

As shown in Fig. 7, the steering screen is constructed by cascading two layers of beam steering devices. Since the steering screen has two layers of active TN LC cells, it can create four polarization statuses in total. In the status 1 shown in Fig. 7(a), both the front and rear TN LC cells are applied with biasing voltages. The incident light directly passes through steering screen without any deflection. In the status 2 shown in Fig. 7(b), only the front TN LC cell is applied with the driving voltage, and the incident light beam is deflected to the left with an angle β_L. In the status 3 shown in Fig. 8(c), the light beam is directly propagated without deflection. In the status 4 shown in Fig. 7(d), no driving voltage is applied to the steering screen, and the incident light beam is deflected to the right with an angle β_R. The deviation angles β_L and β_R can be calculated as follows:

$$\beta_L = \arcsin\left(\frac{n_e \times \alpha}{n_o}\right) - \alpha \approx \frac{(\Delta n) \times \alpha}{n_o} \tag{6}$$

$$\beta_R = \alpha - \arcsin\left(\frac{n_e \times \alpha}{n_o}\right) \approx -\frac{(\Delta n) \times \alpha}{n_o} \tag{7}$$

where $\Delta n = n_e - n_o$ is the birefringence of LC, no and ne are the ordinary and extraordinary refractive indices of the LC respectively, and α is the apex angle of prism array. Thus, a desired deviation angle β can be achieved by choosing an appropriate LC material.

As shown in Fig. 8(a), a measurement platform is built to characterize the steering screen. In this platform, a single wavelength laser pointer (532 nm) is used as the incident light source. A polarizer plate is installed between the light source and the steering screen so that only incident light with a specific polarization direction can pass through. A white board is placed 105 cm from the steering screen to measure the beam projection position. A customized printed circuit-board (PCB) works as the central controller to regulate the steering screen statuses. Measurement results with three deflected light spots on the white board are shown in Fig. 8(b) to (d). In Fig. 8(c), the incident light is directly propagated to the white board at the original position of 9.95 cm when the steering screen is biased in the status 1. In statuses 2 and 4, as shown in Fig. 8(b) and (d), incident light is deflected into positions of 8.25 cm and 11.7 cm respectively. Thus, the deflection angle β can be calculated as below:

$$\beta = \arctan\left(\frac{D}{L}\right) \tag{8}$$

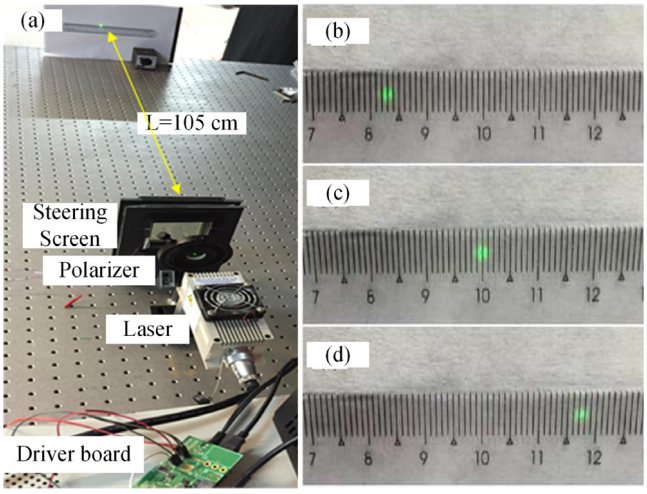

Fig. 8. Test platform on beam steering screen and measurement results.

Table 2
Specifications on AUO M240HW LCD screen.

Parameter	Value
Screen diagonal	609.7 mm
Active area	531.36 mm (H) × 298.89 mm (V)
Pixel resolution	1920 (× 3) (H) × 1080 (V)
Pixel pitch	276.75 μm (per one triad) × 276.75 μm
Pixel arrangement	R.G.B vertical stripe
Display mode	TN mode, Normally white
White brightness	350 cd/cm^2
Contrast ratio	1000
Response time	5 ms
Supply voltage	+5.0 V
Electrical interface	4 Channel LVDS
Color depth	16.7M colors

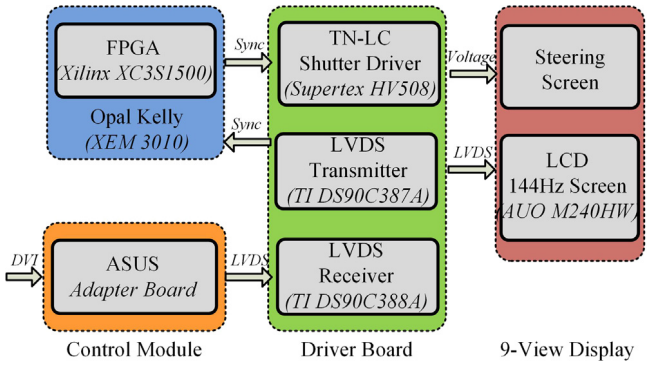

Fig. 9. Schematic diagram on the system circuit driver.

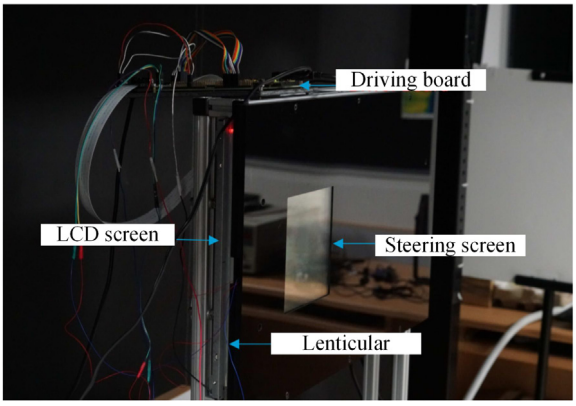

Fig. 10. Photograph of the spatial–temporal multiplexing multi-view display prototype.

where D is the distance between the deflected light spot and the original position, and L is the distance between the white board and the steering screen. Hence, the steering angles for status 2 and status 4 are −0.955° and 0.955° respectively, which closely approximate the desired angle of 0.952°.

5. System integration

A fundamental requirement for the display panel in the proposed multi-view system is that it should be capable of working in a high frame rate condition so as to implement the temporal multiplexing function. In this prototype, an AUO 24-inch 144-Hz TFT-LCD screen is employed as the display panel, and Table 2 summarizes its basic characteristics. In order to synchronize the display panel with the steering screen, as shown in Fig. 9, a PCB is developed to extract the synchronization signal from the video sequence in the image data flow. On this driver circuit board, beside low-voltage-differential-signaling (LVDS) receiver and transmitter chips (TI DS90C388A and DS90C387A), there is a specific liquid crystal driver (Supertex HV508) which regulates biasing voltages on the steering screen. As shown in Fig. 10, the central controller is implemented by an Opal Kelly XEM 3010 field-programmable-gate-array (FPGA) development board. The FPGA module precisely controls the steering screen and synchronizes it with the display panel in parallel.

6. Experimental results

The photograph of the spatio-temporal multiplexing multi-view display prototype for the proof of concept is shown in Fig. 10. In this prototype, the rear LCD screen is fixed on a metal frame, and a customized lenticular sheet is directly attached to it. The steering screen is mounted on the plastic frame in front of the lenticular sheet. As mentioned above, the developed steering screen consists of one piece of TNLC and one piece of LCMPA (including glass, MPA and LC). The size of the TN LC cell was 75 mm × 75 mm × 2.2 mm ($W \times L \times T$), and the thickness of the LCMPA is only 2.9 mm including a 1.8 mm MPA substrate and 1.1 mm glass substrate. The final system employed two pieces of steering screens, which can provide three states. The steering screen and the display panel is attached to each other closely. That is to say, the steering screen was only about 10.2 mm in thickness, which is very compact for 3D display system. The measured transmissivity of one piece of steering screen (including one piece of TNLC and one piece of LCMPA) was 99.1%. Thus, the transmissivity of the steering screen was around 98.2%, which would affect little the display performance. In this prototype, the physical dimension of the steering screen is 150 mm × 150 mm, which covers a 600 × 600 active pixel area, and the remaining area of the LCD panel is disabled in the dark state accordingly.

In this prototype, there are 9 repeating viewing zones created in space by the lenticular sheet, and each viewing zones horizontally covers a 20 mm region. An observer in one viewing zone can only see a monochrome R, G, B image at any moment. Due to temporal multiplexing from the steering screen, the observer continuously views separate R, G, B images so as to perceive a full color image. Similar to the experimental set-up mentioned in Section 3, the Eldim VCmaster 3D analyzer was also employed to measure the angular luminance distribution over the entire viewing field. Since the system is based on the temporal multiplexing method, the viewer will observe three states of multi-view sequentially in a high speed. During the measurement process, the Eldim VCmaster 3D analyzer measured the luminance distribution for nine views in three states. The final distribution can

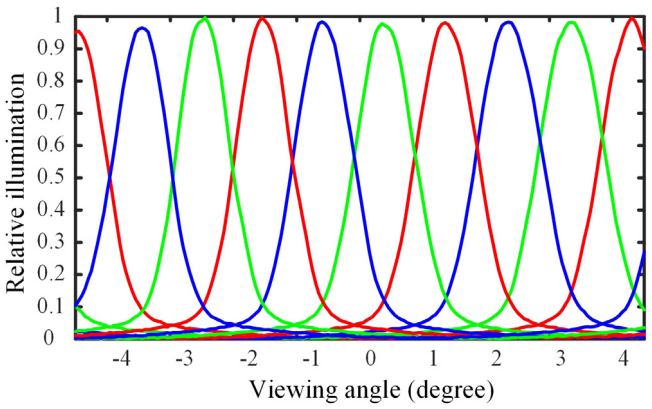

Fig. 11. Angular luminance distribution for nine views of the developed spatio-temporal multiplexing multi-view display system. (For interpretation of the references to color in this figure legend, the reader is referred to the web version of this article.)

Fig. 12. Photographs taken in the viewing position V_5 during a complete display cycle. (For interpretation of the references to color in this figure legend, the reader is referred to the web version of this article.)

be obtained by averaging the three groups of distribution, which is shown in Fig. 11. Based on the above definition of crosstalk, the averaged crosstalk for these selected nine views is 25.1%, and the largest crosstalk among the nine views is 28.4%. Compared with the ones of the multi-view display with lenticular, the introducing of beam steering screen increases the number of views while affecting little the display performance. An experiment was also set up to show the performance, multiple stereo images are prepared by taking photos in a real scene from 9 different viewing directions with calibrations, and they are merged together to generate a super image which is further split into three subframes so as to synchronize with the steering screen in time domain. Fig. 12 shows experimental results in the viewing position V_5 during a complete display cycle. It shows that green, red and blue images are sequentially projected to this viewing position, which verifies the effectiveness of the spatial and temporal multiplexing. Since the rear LCD screen works in a speed of 120 Hz, the equivalent refresh rate of each monochrome image is 40 Hz, which can meet the persistence of vision.

7. Conclusion

In this paper, a spatio-temporal multiplexing multi-view 3D display with horizontal stereo and motion parallax is proposed. The 3D display system comprises a fast liquid-crystal-display (LCD), a lenticular lens sheet and a beam steering screen. Spatial multiplexing is implemented by the customized lenticular sheet which horizontally splits the display image on the LCD screen into separate viewing zones so as to achieve stereo and motion parallax in parallel. The steering screen implements temporal multiplexing by sequentially deflecting the light beam split from the lenticular lens into three desired directions. The observer at a given viewing position perceives a full color image by successively viewing R, G, B images within a complete display cycle. An experimental prototype based on the proposed technology is evaluated for the proof of concept, and testing results show the effectiveness on spatio-temporal multiplexing.

Funding

National Research Foundation of Singapore, Competitive Research Program (NRF-CRP11-2012-01).

References

[1] D. Cheng, Y. Wang, H. Hua, M. Talha, Design of an optical see-through head-mounted display with a low f-number and large field of view using a freeform prism, Appl. Opt. 48 (14) (2009) 2655–2668.
[2] D. Smalley, Q. Smithwick, V. Bove, J. Barabas, S. Jolly, Anisotropic leaky mode modulator for holographic video displays, Nature 498 (7454) (2013) 313–317.
[3] F. Yaraş, H. Kang, L. Onural, Circular holographic video display system, Opt. Express 19 (10) (2011) 9147–9156.
[4] D. Miyazaki, K. Shiba, K. Sotsuka, K. Matsushita, Volumetric display system based on three-dimensional scanning of inclined optical image, Opt. Express 14 (26) (2006) 12760–12769.
[5] W. Song, Q. Zhu, T. Huang, Y. Liu, Y. Wang, Volumetric display based on multiple mini-projectors and a rotating screen, Opt. Eng. 54 (1) (2015) 013103-1–013103-6.
[6] X. Xia, X. Liu, H. Li, Z. Zheng, H. Wang, Y. Peng, W. Shen, A 360-degree floating 3d display based on light field regeneration, Opt. Express 21 (9) (2013) 11237–11247.
[7] Q. Zhong, Y. Peng, H. Li, C. Su, W. Shen, X. Liu, Multiview and light-field reconstruction algorithms for 360 multiple-projector-type 3d display, Appl. Opt 52 (19) (2013) 4419–4425.
[8] N.-Y. Jo, H.-G. Lim, S.-K. Lee, Y.-S. Kim, J.-H. Park, Depth enhancement of multi-layer light field display using polarization dependent internal reflection, Opt. Express 21 (24) (2013) 29628–29636.
[9] C.-H. Chen, Y.-P. Huang, S.-C. Chuang, C.-L. Wu, H.-P.D. Shieh, W. Mphep¨o, C.-T. Hsieh, S.-C. Hsu, Liquid crystal panel for high efficiency barrier type autostereoscopic three-dimensional displays, Appl. Opt. 48 (18) (2009) 3446–3454.
[10] H. Yamamoto, M. Kouno, S. Muguruma, Y. Hayasaki, Y. Nagai, Y. Shimizu, N. Nishida, Enlargement of viewing area of stereoscopic full-color led display by use of a parallax barrier, Appl. Opt. 41 (32) (2002) 6907–6919.
[11] W. Song, Q. Zhu, Y. Liu, Y. Wang, Omnidirectional-view three dimensional display based on rotating selective-diffusing screen and multiple mini-projectors, Appl. Opt. 54 (13) (2015) 4154–4160.
[12] E. Buckley, A. Cable, N. Lawrence, T. Wilkinson, Viewing angle enhancement for two-and three-dimensional holographic displays with random superresolution phase masks, Appl. Opt. 45 (28) (2006) 7334–7341.
[13] S. Jiao, X. Wang, M. Zhou, W. Li, T. Hong, D. Nam, J.-H. Lee, E. Wu, H. Wang, J.-Y. Kim, Multiple ray cluster rendering for interactive integral imaging system, Opt. Express 21 (8) (2013) 10070–10086.
[14] F. Yi, J. Lee, I. Moon, Simultaneous reconstruction of multiple depth images without off-focus points in integral imaging using a graphics processing unit, Appl. Opt. 53 (13) (2014) 2777–2786.
[15] Y.-H. Tao, Q.-H. Wang, J. Gu, W.-X. Zhao, D.-H. Li, Autostereoscopic three-dimensional projector based on two parallax barriers, Opt. Lett. 34 (20) (2009) 3220–3222.
[16] G.-J. Lv, J. Wang, W.-X. Zhao, Q.-H. Wang, Three-dimensional display based on dual parallax barriers with uniform resolution, Appl. Opt. 52 (24) (2013) 6011–6015.
[17] Y.-G. Lee, J.B. Ra, Image distortion correction for lenticula misalignment in three-dimensional lenticular displays, Opt. Eng. 45 (1) (2006) 017007–017007.
[18] Z. Zhuang, P. Surman, X.W. Sun, F. Yu, Flat-concave dual-mirror configuration design for upright projection-type ultrashort throw ratio projectors, J. Disp. Technol. 12 (1) (2016) 8–16.
[19] R.S. Brar, P. Surman, I. Sexton, R. Bates, W.K. Lee, K. Hopf, F. Neumann, S.E. Day, E. Willman, Laser-basedhead-tracked 3d display research, J. Disp. Technol. 6 (10) (2010) 531–543.
[20] Z. Zhuang, L. Zhang, P. Surman, S. Guo, B. Cao, Y. Zheng, X.W. Sun, Directional view method for a time-sequential autostereoscopic display with full resolution, Appl. Opt. 55 (28) (2016) 7847–7854.